Hyperspectral estimation models for nitrogen contents of apple leaves

LI Bingzhi, LI Minxia, ZHOU Xuan, ZHANG Linsen, ZHANG Haiyan

College of Horticulture, *Northwest Agriculture & Forest University*, *Shaanxi YangLing* 712100, *China*

Abstract: Plant nitrogen status is a key indicator for evaluating crop growth, increasing yield and improving grain quality. Non-destructive and rapid assessment of leaf nitrogen is required for improving nitrogen management in fruit tree production. The hyperspectral reflectance and corresponding total nitrogen concentration of different species of apple trees' leaves were measured by Field-Spec PMI-MASTER PRO. The correlation among raw hyperspectral reflectance, first derivative spectra, and hyperspectral characteristic variables were analyzed. This paper makes a model for the quantitative detection of leaf's total nitrogen with a view to providing a theoretical foundation for nutrition diagnosis of the apple by remote technology. The results showed that the raw spectral reflectance has the maximum negative correlation coefficient at 715nm ($r = -0.817$) with total nitrogen concentration and the logarithm model constructed with reflectance at this point is the better one as compared to linear model; the first derivative spectral reflectance has the maximum positive correlation coefficient at 723nm ($r = 0.87$) and the linear and non-linear models have the similar capacity for the nit rogen est imation; as to hyperspectral characteristic variables, they all show significant correlation with nitrogen contents except λy, SD /SDy and (SDr + SDy)/(SDr − SDy). Those results indicate that the variables adopt in this paper have great potential for nitrogen concentration test. By the precision evaluation of estimation models, the logarithm model constructed by the first derivative reflectance at 723 nm was proved to be the best for the estimation of apple leaves nitrogen concentration.

Key words: apple, spectral parameter, leaf total nitrogen concentration, monitoring model

CLC number: 0433.1/TP79 **Document code:** A

Citation format: Li B Z, Li M X, Zhou X, Zhang L S and Zhang H Y. 2010. Hyperspectral estimation models for nitrogen contents of apple leaves. *Journal of Remote Sensing*. **14**(4): 761—773

1 INTRODUCTION

Nitrogen (N) is the most demanding nutrient element for fruit tree growth, and significantly affects photosynthetic production and yield formation in fruit trees. Thus N fertilization has become one of main yield-enhancing techniques in modern crop production. Plant nitrogen accumulation, as a product of plant nitrogen content and plant mass, strongly affects yield and quality formation in fruit production. Since nitrogen fertilization strategy is a major consideration in field management and proper strategy should ensure N supply at the right time and appropriate amount, it is necessary to evaluate tissue N status and recommend N dressing plan from indicative nitrogen content and nitrogen accumulation in plants.

Effective diagnosis and dynamic regulation of plant N status must be based on real-time monitoring of growth characters and nitrogen levels in plants. Until now, traditional method of measuring crop N status depends on plants sampled from fields and chemical assays in laboratories, which could not meet the need of rapid, real-time and nondestructive monitoring and effective diagnosis of plant N status. The newly-emerged hyper-spectral remote sensing makes possible acquiring images in many narrow and continuous spectral bands, which are sensitive to specific plant variables, so weak difference in plant parameters could be detected. Extracting sensitive bands and converting spectral parameters to reduce background effects can help to improve the level and quality of capturing crop growth information, so hyper-spectral remote sensing technology can be used to better estimate various growth variables related to plant physiology and biochemistry (Vane, 1993). The canopy spectra obtained via remote sensing reflect complex information of vegetation including the leaves, stems, spikes, soils and other backgrounds. To accurately extract characteristic information from targets and trace its subtle change, the derivative spectral data were calculated to minimize spectral noise caused by the soil background and atmospheric effects. Hyperspectral sensors measure reflectance in a large number of narrow wavebands, generally with bandwidths of less than 10nm. With these narrow bands, reflectance and absorption features related to specific plants physical and chemical characteristics can be detected (Takebe, 1990; Thomas *et al*., 1972; Everitt *et al*., 1987; Yoder, 1995; Blackmer *et al*., 1996; Stone

Received: 2009-09-09; **Accepted**: 2009-10-13

Foundation: National Science and Technology supporting plan (No. 2007BAK31B01); National Modern Agricultural (Apple) Industry Technology System; Agriculture Ministry 948 Project (No. 2006-G28).

First author biography: LI Bingzhi (1956—), male, Professor. He graduated from the College of Horticulture of Northwest A&F University. He is working on fruit tree physiology and ecology. He has published 23 books and 28 papers. E-mail: bzhli530530@163.com

et al., 1996; Tarpley *et al.*, 2000; Xue *et al.*, 2004).

Leaf nitrogen accumulation, as a product of leaf nitrogen content and leaf mass, includes not only nitrogen content information, but also canopy coverage properties. Leaf N content and canopy coverage increase with N fertilizer increasing, which promotes rapid increment of leaf N accumulation (Zhu *et al.*, 2006; Wang *et al.*, 1993). The differences in soil fertility levels and cultural management practices in the fields often result in apparent heterogeneous growth among individual plants in plant population, which severely affects yield and quality formation in fruit production. Therefore, monitoring LNA and dynamic changes is useful to evaluate plant production capability and predict yield and quality. Determining quantitative relationship of canopy spectra with LNA should help to support non-destructive and real-time monitoring and diagnosis of N status in fruit production. The objective of the present study was to analyze relationship between canopy reflectance spectra and leaf N status in apple trees on the basis of field experiments involving different N rates and cultivars in growing seasons, to calculate general equations from different data sets for predicting N nutrition index in apple. The anticipated results would help to provide a technical approach for non-destructive and real-time monitoring of N nutrition status in apple trees.

2 MATERIALS AND METHODS

2.1 Design of experiments

The data were obtained from 3 field experiments involving different N fertilization rates and apple cultivars.

Experiment 1: The experiment was carried out at the apple experiment station located at Baoji Fengxiang County from 2007 to 2008 with 6 treatments and 3 replicates. The soil in the fields was sandy silt soil with 2.09g·kg^{-1} organic matter, 0.18g·kg^{-1} total N, 120.20mg·kg^{-1} available N, 110.03mg·kg^{-1} available phosphate (P_2O_5) and 83.5mg·kg^{-1} available potassium (K_2O). 2 cultivars were selected: Lifu No.1 and Gala. 3 N rates were applied: N_1, 0kg N·hm^{-2}; N_2, 320kg N·hm^{-2}; N_3, 640kg N·hm^{-2}. N application was distributed in 3 splits: bloom in April, fruit development in June and fruit enlargement in July. Other management followed local standard practices. Apple leaves were determined for spectra and total nitrogen in July, September and October. The experiment data were used for testing models.

Experiment 2: The experiment was carried out at Dong Guizhuan's apple orchard located at Baoji Fengxiang County from 2007 to 2008 with 6 treatments and 3 replicates. The soil in the fields was sandy silt soil with 1.43g·kg^{-1} organic matter, 0.11g·kg^{-1} total N, 62.5mg·kg^{-1} available N, 10.36mg·kg^{-1} available phosphate (P_2O_5) and 62.5mg·kg^{-1} available potassium (K_2O). 2 cultivars were selected: Red Fuji and Qinguan. 3 N rates were applied: N_1, 0kg N·hm^{-2}; N_2, 345kg N·hm^{-2}; N_3, 690kg N·hm^{-2}. N application was distributed in 3 splits: bloom in April, fruit development in June and fruit enlargement in July. Other management followed local standard practices. Apple leaves were determined for spectra and total nitrogen in July, September and October. The experiment data were used for testing models.

Experiment 3: The experiment was carried out at Huo Zhiwen's apple orchard located at Baoji Fengxiang County from 2007 to 2008 with 6 treatments and 3 replicates. The soil in the fields was sandy silt soil with 1.75g·kg^{-1} organic matter, 0.52g·kg^{-1} total N, 81.20mg·kg^{-1} available N, 74.03mg·kg^{-1} available phosphate (P_2O_5) and 81.51mg·kg^{-1} available potassium (K_2O). 2 cultivars were selected: Red Fuji and Qinguan. 3 N rates were applied: N_1, 0kg N·hm^{-2}; N_2, 345kg N·hm^{-2}; N_3, 690kg N·hm^{-2}. N application was distributed in 3 splits: bloom in April, fruit development in June and fruit enlargement in July. Other management followed local standard practices. Apple leaves were determined for spectra and total nitrogen in July, September and October. The experiment data were used for testing models.

2.2 Spectra measurement

All spectral measurements were taken under clear sky conditions between 10:00 and 14:00 (Beijing local time), using an ASD Field Spec Pro spectrometer (Analytical Spectral Devices, Boulder, CO, USA). This spectrometer is fitted with a 25° field of view fiber optics, operating in the 325–1075nm spectral region with a sampling interval of 1.5nm. A 40cm×40cm $BaSO_4$ calibration panel was used for calculating the black and baseline reflectance. Vegetation radiance measurement was taken by averaging 20 scans at an optimized integration time, with a dark current correction at every spectral measurement (Min *et al*., 2008). A panel radiance measurement was taken before and after the vegetation measurement by two scans each time. In each experiment, data were obtained on several different backgrounds (dark cloth, white paper and soil).

2.3 Determination of leaf N status

After each measurement of spectral reflectance, 7 plants about 350 leaves from each plot were collected for determination of leaf weight and leaf N concentration. All the samples were cleaned by distilled water, fixation at 105℃ for 10—15min, then oven-dried at 80℃ to constant weight. The dried leaf samples were ground to pass through a 1mm screen, and then stored in plastic bags for chemical analysis. Total N concentration in leaf tissues was determined by the micro-Keldjahl method. Leaf N concentration (LNC, g 100 g^{-1}) was expressed on the basis of unit leaf dry weight. It was determined by the equation as follows

$$\mathrm{N}(\%)=\frac{(V-V_0)\times C_{\mathrm{H}}\times 0.014}{m}\times 100\%$$

where V is the volume of used standard acid, V_0 is the volume of blank standard acid, C_{H} is concentration of the standard acid, and m is weight of the dried leaves.

2.4 Data analysis and use

The data from Experiments 1 were used for deriving equations to predict N nutrition index in apple tree Table 1, and the data from Experiment 2 and 3 were used for testing the derived equations. Correlation analyses were conducted between the hyperspectral parameters and LNC so that sensitive spectral ranges (known as key bands) and spectral indices reported related to LNC were identified in apple tree (Pu & Gong, 2000; Guyot & Baret, 1988; Richardson & Wiegand, 1977; Pearson & Miller, 1972). Nine spectral parameters selected were calculated according to the equations in Table 2. Separate linear models were fitted to determine the best-fit R^2 values for the relationships of LNC to the spectral parameters. The relationships with the best-fit R^2 values were tested with the data from Experiment 1. In equation testing, the predicted results were compared with the field measurements to evaluate reliability and accuracy of the equation output under practical conditions. The following statistic method, root mean square error (RMSE) and mean relative error (RE) was used to calculate the fitness between the estimated results and observed data.

Table 1 Definition of hyperspectral remote sensing parameters used in the study

Type	Spectral parameter	Definition
Characteristic variable based on spectral position	Dr	The first order maximal derivative inside red edge
	λr	Corresponding band length with D_r
	Db	The first order maximal derivative inside blue edge
	λb	Corresponding band length with D_b
	Dy	The first order maximal derivative inside blue edge
	λy	Corresponding band length with D_y
	Rg	Spectral reflectance at green band peak
	λg	Corresponding band length with R_g
	Ro	Spectral reflectance at red band peak
Characteristic variable based on spectral area	SDr	Summation of the first order derivation inside red edge
	SDb	Summation of the first order derivation inside blue edge
	SDy	Summation of the first order derivation inside yellow edge
Characteristic variable based on vegetation index	SDr/SDb SDr/SDy Rg/Ro	Ratio vegetation index
	(SDr−SDb)/(SDr+SDb) (SDr−SDy)/(SDr+SDy) (Rg−Ro)(Rg+Ro)	Normalized difference vegetation index

Table 2 Correlation coefficient between nitrogen content and hyperspectral variables

	Types of spectral parameters	*r*
Spectral parameters based on position	Db	−0.855
	λb	0.752
	Dr	−0.818
	λr	0.876
	Dy	−0.830
	λy	0.147
	Rg	−0.808
	λg	0.721
	Ro	−0.741
Vegetation indexes	SDr/SDb	0.874
	SDr/SDy	−0.129
	Rg/Ro	−0.647
	(SDr−SDb)/(SDr+SDb)	0.853
	(SDr−SDy/(SDr+SDy)	−0.256
	(Rg−Ro)/(Rg+Ro)	−0.641
Spectral parameters based on area	SDr	−0.806
	SDb	−0.839
	SDy	0.725

3 RESULTS AND ANALYSIS

3.1 Apple leaves hyperspectral reflectance under different N rates

The hyperspectral reflectance of apple leaves over different growth stages was markedly different under varied N rates. Fig. 1 displays the response patterns of leaves reflectance spectra to the N rates Fig. 1(a) and different development stages Fig. 1 (b) of Lifu No.1. In the visible wavebands (400—710nm), the hyperspectral reflectance was lower at higher N rates, whereas in the NIR wavebands (760—1000nm) the reflectance tended to increase with increasing N rate, resulting in greater differences among the N rates in NIR short wave bands than that in visible wave bands. This indicates that the reflectance in the NIR region was responsive to growth status of apple tree under different N rates, but tended to be saturating under high N rates.

As shown in Fig. 1(b), effects of development stages on reflectance spectra presented the same regularity as LNA in 500—700 nm and 750—1000 nm. Plants rapidly grew to boost N absorption and cover increment from fruit development to fruit enlargement. So canopy structure and biochemical variables in apple tree differed significantly among growth stages, which would result in changes of spectral properties at canopy level, with the reflectance in the visible wavebands decreasing with growth stages and increasing in the NIR region.

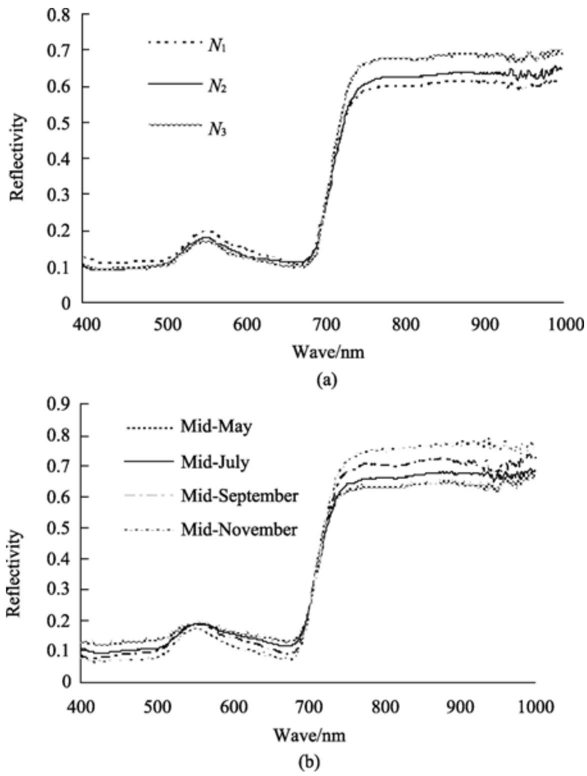

Fig. 1 Changes in spectral reflectance (a) and different development stages (b) of apple with varied leaf nitrogen concentration

3.2 Relationships of leaf total N concentration to the spectral reflectance

Fig. 2 illustrates the correlation between the spectral reflectance of all spectral bands and its first derivative spectra and LNA from the pooled data (n=216). As shown in Fig. 2, LNA were negatively related to the reflectance in visible wavebands (400—700nm), with the lowest correlation coefficients in 650—700 named red valley induced by chlorophyll absorption, while LNA were positively related to the reflectance in NIR region (760—1000nm), with the highest correlation coefficients r = 0.788 because of high green leaf biomass and area induced by N supply. In particular, the spectral bands in 700—750nm were within a region of red edge, where correlation coefficients changed rapidly around 715nm, so 715nm was named red edge inflexion. In the red edge region, capability of radiation absorption by chlorophyll decreased gradually, and capability of radiation reflection through mesophyll cell structure increased with band shifting to long wave. The highest correlation coefficient (r = –0. 817) was found at about 715nm.

Took the spectral reflectance of 715nm as independent variable, leaf total N concentration as attributive variable, 2 regression equations were obtained (Fig.3). Coefficients of determination (R^2) from the power equation of FD715 to LNA were above 0.7, indicating that the 2 regression equations well described the dynamic pattern of LNA changes in apple leaves.

3.3 Relationships of leaf total N concentration to the first derivative spectral reflectance

Fig. 4 shows that correlation coefficients between the first derivative spectra and LNA were negative in 550—600 nm named blue edge region with most significant level of –0.84, and positive in 700—750 nm named red edge region with the highest correlation coefficients of 0.87 at 723 nm reaching extremely significant levels. Canopy spectral reflectance in red edge region was sensitive to biomass and LAI changed rapidly, which led to significant correlation of its derivative spectra to LNA.

Took the first derivative spectral reflectance of 723 nm as independent variable, leaf total N concentration as attributive variable, 2 regression equations were obtained (Fig.5). Coefficients of determination (R^2) from the power equation of FD723 to LNA were above 0.7, indicating that the 2 regression equations well described the dynamic pattern of LNA changes in apple leaves.

3.4 Relationships of leaf N accumulation to hyperspectral parameters

As shown in Table 2, except yellow edge (λy), all the other parameters reached the significant correlation with total N concentration. Blue edge, red valley and λg all reached the significant level. Among the vegetation indexes, except the ratio of SDr/SDy, all the other parameters had significant correlation with total N concentration. This means it is feasible to use these parameters to evaluate total N concentration. Based on the linear and exponential models of Dr, Db and Dy (Table 3), the coefficients of determination of the exponential model are higher than the linear model. The model based on λr has the highest coefficients of determination and the similar effect of both the linear and exponential models. But in contrast to exponential model, linear model is easier, so we chose model y=43.391x –0.1467 to predict the total N concentration and tested its precision.

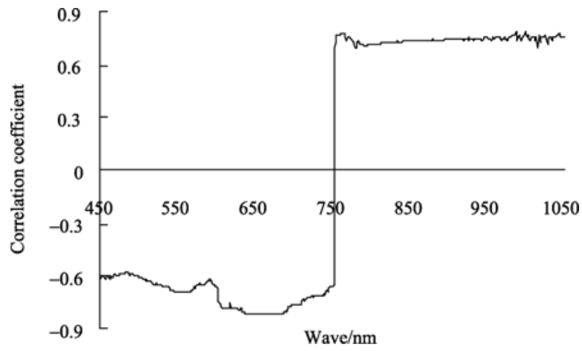

Fig. 2 Correlation between the leaf total nitrogen concentration and the spectral reflectance

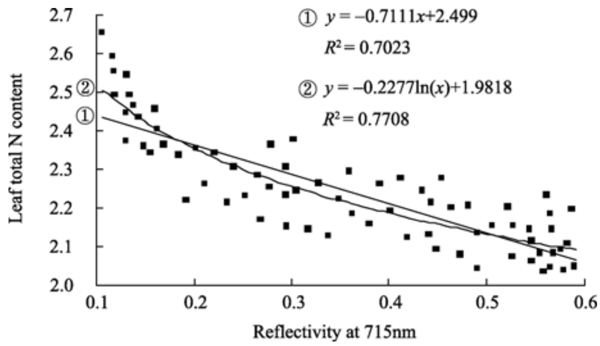

Fig. 3 Regression relationship between leaf total nitrogen content and the characteristic leaf reflectance at 715nm

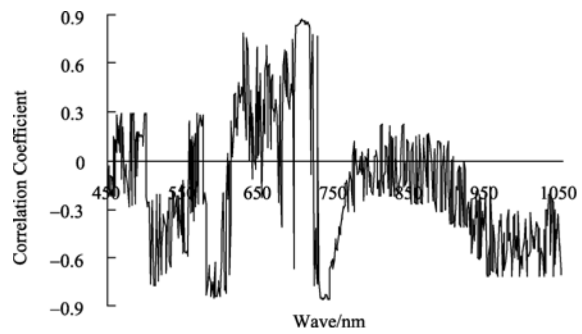

Fig. 4 Correlation between the total nitrogen concentration and the first derivative spectral reflectance

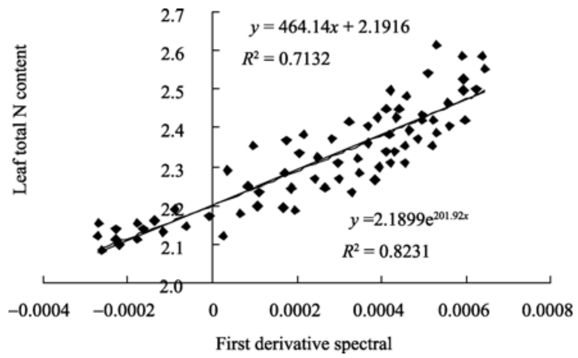

Fig. 5 Regression relationship between leaf total nitrogen content and the characteristic leaf reflectance at 723nm

3.5 Test and verification of models

In order to test whether these regression models were reliable

Table 3 Quantitative relationships of leaf total nitrogen content (*y*) to spectral parameters (*x*) in apple

Spectral parameters	Model	Regression equation	R^2
D_r	Linear	$y=-156.78x+3.643$	0.649
	exponential	$y=4.854x^{-70.495}$	0.671
D_b	Linear	$y=6.188x-340.22$	0.720
	exponential	$y=4.357x^{-180.66}$	0.715
D_y	Linear	$y=3.022x-2299.3$	0.737
	exponential	$y=3.195e^{-1256.3x}$	0.764
λ_r	Linear	$y=43.391x-0.1467$	0.848
	exponential	$y=6.5e^{-0.027x}$	0.840
λ_b	Linear	$y=-126.71x+0.248$	0.523
	exponential	$y=6.8e^{-310.135x}$	0.534
R_g	Linear	$y=3.359x-6761$	0.633
	exponential	$y=3.777e^{-361x}$	0.641
λ_g	Linear	$y=229.678x-0.41$	0.472
	exponential	$y=1.4e^{-0.232x}$	0.542
R_o	Linear	$y=3.276x-9648$	0.548
	exponential	$y=3.646e^{-5.218x}$	0.547
SD_r	Linear	$y=3.802x-4786$	0.672
	exponential	$y=4.781x^{-2.553}$	0.658
SD_b	Linear	$y=3.088x-11.021$	0.717
	exponential	$y=3.272x^{-5.892}$	0.705
SD_r/SD_b	Linear	$y=0.133x-0.452$	0.765
	exponential	$y=0.590x^{0.2396}$	0.746
$(SD_r-SD_b)/(SD_r+SD_b)$	Linear	$y=-2.113x-6.614$	0.737
	exponential	$y=0.590x^{-0.2396}$	0.725

and applicable for LNA estimation, the independent data set from Exp. 2 and 3 were used to test the performance of these models. Root mean square error (RMSE), average relative error (RE), and precision (R^2) were employed to test the reliability between the estimated values and the measured values, as shown in Table 4. Also comparison of estimated with measured leaf nitrogen accumulation in apple tree was shown in Fig. 6.

Table 4 Comparison of precision test results of hyperspectral models for total nitrogen content (n = 72)

Independent variable *x*	Model	R^2	RMSE	RE
$\rho715$	$y=-0.2277\ln(x)+1.9818$	0.771**	0.377	17.7
$\rho723$	$y=2.1899e^{201.92x}$	0.879**	0.245	9.86
λr	$y=43.391x-0.14$	0.848**	0.302	12.46
SDr/SDb	$y=0.133x-0.452$	0.759**	0.370	16.78

Note: * and ** stand for the significances at significant and high significant levels, respectively.

The results showed that these variables gave good explanation of changes in total N. But considering the uncertainty of changes in parameters caused by one variable, the uniqueness should be considered as well. Based on the rules mentioned above, the leaf reflectance at 715nm and the first derivative spectral reflectance of 723nm were suitable. For the idea model we chose as the first derivative spectral reflectance of 723nm had the highest coefficients of determination, lowest RMSE and RE.

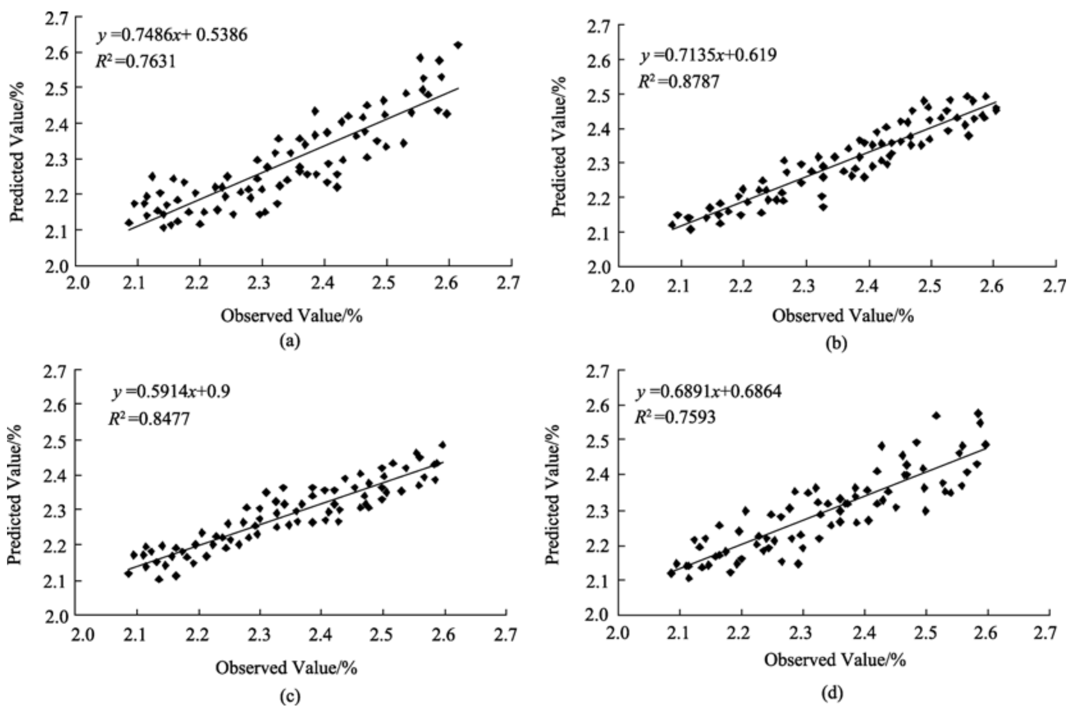

Fig. 6 Comparison between the predicted value and the measured value of total nitrogen content of apple
(a): Lifu No.1 in 2007; (b): RoyalGala in 2007; (c): Lifu No.1 in 2008; (d): QinGuan in 2008

4 DISCUSSION

In this study, hyperspectral remote sensing estimation of total nitrogen content in apple leaves was used, which is a non-destructive testing technology, that is, without undermining the organizational structure of plant leaves, using spectrometer measured spectral reflectance characteristics of changes in leaf nitrogen. Compared to the traditional biochemical analysis, remote sensing is not only the in vivo observations, but also decreases the analysis costs. This paper analyzed the quantitative relationship between the total nitrogen content in apple leaves and leaf spectral characteristics, based on the sensitive bands of nitrogen, established the monitoring model of the total nitrogen content in apple leaves on the red edge position (λr). The results showed that the goodness of fits of two-band combined spectral variables and total N was much higher than that of a single band. This was the same as the study of Daughtry *et al.* (2000). The reason probably is that the single band spectrum is easier confused by the reflectance of background or leaf area index. Thus several techniques and methods have been used to minimize spectra noise, such as derivative spectra and new vegetable indices. Rondeaux *et al.* (1996) proposed OSAVI to reduce soil background noise. Gitelson *et al.* (2002) calculated VARI to revise atmospheric effects on spectra. Demetriades-shah *et al.* (1990) suggested that derivative spectra indices not only minimized background noise, but also resolved mixed spectra. The present study adopted different methods to parameterize the red edge position (REP) in relation to spectral shift. Miller *et al.* (1990) employed an inverted Gaussian model to calculate REP, and found a close correlation between REP and chlorophyll concentrations. Cho and Skidmore (2006) reported the linear extrapolation method for extracting REP from hyperspectral data that aims to mitigate the discontinuity in the relationship between the REP and the nitrogen content caused by the existence of a double-peak feature on the derivative spectrum. Compared to the existing N sensitive bands and vegetation indices, the index combines information on visible band, is easy to access and provide information of a portable monitor for nitrogen spectra testing.

Spectral data obtained in this paper was only from Fengxiang Country. In future studies, we should expand sampling areas and set different yield and nitrogen levels to explore the potential of using hyperspectral remote sensing estimation of total nitrogen content in apple leaves in order to provide theoretic evidence for the management of orchard.

5 CONCLUSIONS

The precision agriculture depends on timely and rational nitrogen application by real-time monitoring of crop growth parameters and plant N status. The leaf nitrogen concentration can well indicate N nutrition status in plant, so a number of studies have been made to estimate the LNC with multi-spectral reflectance. As compared to the multiple spectral reflectance used in previous studies, the hyperspectral reflectance adopted in the present study is generally more sensitive to specific plant variables because of acquiring abundant information in narrow and continuous spectral bands. The quantitative relationships of the leaf N indices to the hyperspectral parameters of canopy reflectance in apple trees were comprehensively analyzed using field experiment data involving different N rates and cultivars in this paper. The results showed that the hyperspectral reflectance was lower at higher N rates in the visible wavebands, whereas the reflectance tended to increase with increasing N rate in the NIR wavebands. The reflectance in the visible wavebands decreased with growth stages and increase in the NIR region. The highest correlation coefficient (r = –0. 817) between the leaf total nitrogen concentration and the spectral reflectance was found at about 715nm whereas the highest correlation coefficients between the total nitrogen concentration and the first derivative spectral reflectance of 0.87 at 723nm reaching extremely significant levels. The exponential models were better than the linear models but for the first derivative spectral reflectance both models were good. For the idea model we chose as the first derivative spectral reflectance of 723nm had highest coefficients of determination, lowest RMSE and RE.

REFERENCES

Blackmer T M, Schepers J S and Varvel G E. 1996. Nitrogen deficiency detection using reflected short wave radiation from irrigated corn canopies. *Agronomy Journal*, **88**(1): 1—5

Cho M A and Skidmore A K. 2006. A new technique for extract in the rededge position from hyperspectral data: the linea extra polation method. *Remote Sensing of Environment*, **101**(2): 181—193

Daughtry C S T, Walthall C L and Kin M S. 2000. Estimatin corn leaf chlorophyll concentration from leaf and canop reflectance. *Remote Sensing of Environment*, **74**: 229—239

Everitt J H, Pettit R D and Alaniz M A. 1987. Remote sensing of broom snake weed (Gutierrezia sarothrae) and spinyaster (Asterspo-sus).*Weed Science*, **35**(2): 295—302

Guyot G and Baret F. 1988. Utilisation dela haute resolutio spectrale poursuivrel'etatdes couverts vegetaux.Proceedings of the Fourth International Conference on Spectral Signatures of Objects in Remote Sensing, Assois(France): European Space Agency

Miller J R. 1990. Quantitative Characterization of the Vegetation Red Edge Reflectance.An Inverted Gauss Ian. Reflectance Model. *International Journal of Remote Sensing*, (11): 1775—1795

Min Min, Won Suk Lee, Thomas F Burks, Jonathan D Jordan, Arnold W Schumann, John K Schueller and Huikai Xie. 2008. Design of a hyperspectral nitrogen sensing system for orange leaves. *computers and electronics in agriculture*. **63**: 215—226

Pearson R L and Miller D L. 1972. Remote mapping of stand in crop biomass for estimation of the productivity of the shortgrass prairie. Proceedings of the Eighth Interntional Symposium on Remote Sensing of Environment. Michigan: Environmental Research Institute of Michigan

Pu R and Gong P. 2000. Hyperspectral remote sensing and its application. Beijing: Higher Education Press

Richardson A J and Wiegand C L. 1977. Distinguishing vegetation from soil background information. *Photogramm Engineering and Remote Sensing*, **43**: 1541—1552

Rondeaux G, Steven M and Baret F. 1996. Optimization of soiladjusted vegetation indices. *Remote Sensing of Enviroment*, **55**: 95—107

Stone M L, Solie J B, Rrun W R, Whitneey W, Taylor S L and Ringer J D. 1996. Use of spectral radiance for correcting in-season fertilizer nitrogen deficiencies in winter wheat. *Transactions of ASAE*, **39**: 1623—1631

Takebe M, Yoneyama T, Inada K and Murakami T. 1990. Spectral reflectance ratio of rice canopy for estimating crop nitroge status. *Plant Soil*, **122**: 295—297

Tarpley L, Redd K R and Sassenrath Cole G F. 2000. Reflectance indices with precision. *Crop Science*, **40**: 114—119

Thomas J R and Oerther G F. 1972. Estimating nitrogen content of swepepper leaves by reflectance measurements. *Agronom Journal*, **64**: 11—13

Vane G. 1993. Terrestrial imaging spectro metry: Current status, future trends. *Remote Sensing of Environment*, **44**(2): 109—127

Wang C R, Chen M Z and Jiang H X. 1993. Study on the agricultural mechanism of yield estimation using remote sensing: Spectral characteristics of rice with different nitrogen level and selection of sensitive waveband. *Journal of Zhejiang Agricultural University*, **19**(Suppl): 7—14

Xue H L, Cao W X, Luo W H and Zhang X.2004.Correlation between leaf nitrogen status and canopy spectral characteristics in wheat. *Acta Phytoecologica Sinica*, **28**(2): 172—177

Yoder B J and Pettingew Crosby R E. 1995. Predicting nitrogen and chlorophyll concentrations from reflectance spectra (400—2500nm) at leaf and canopy scales. *Remote Sensing of Environment*, **53**: 199—211

Zhu Y, Li Y X, Zhou D Q, Tian Y C, Yao X and Cao W X. 2006. Quantitative relationship between leaf nitrogen concentration and canopy reflectance spectra in rice and wheat. *Acta Ecologica Sinica*, **26**(10): 3463—3469

苹果树叶片全氮含量高光谱估算模型研究

李丙智, 李敏夏, 周　璇, 张林森, 张海燕

西北农林科技大学园艺学院 陕西 杨凌 712100

摘　要: 采用 Field-Spec Pro 便携式光谱仪, 测定了不同苹果品种叶片的光谱反射率及对应的全氮含量, 采用相关性及单变量线性与非线性拟合分析技术, 对全氮含量与原始光谱反射率、一阶微分光谱、高光谱参数之间的关系进行了分析。研究确立叶片全氮含量的定量监测模型, 以期为遥感技术在苹果氮素营养诊断中的实际应用提供理论依据。结果表明: 全氮含量与原始光谱在 715nm 处具有最大负相关系数(r = –0. 817), 并且基于此波长所构建的对数关系估算模型明显优于线性模型; 光谱反射率一阶微分值在 723nm 处具有最大正相关系数(r = 0.87), 并且基于此波长所构建的线性和非线性模型的拟合效果接近; 对于所选取的 3 类高光谱特征变量, 全氮含量除了与黄边位置及由红边位置和黄边面积所构建的比值植被指数和归一化植被指数的相关性较弱外, 与其余变量均呈极显著相关, 说明这些变量对苹果叶片全氮含量进行估算具有可行性。对所建立的各类方程进行检验, 最终筛选确定在 723nm 处的光谱反射率一阶微分值所构建的指数模型作为苹果叶片全氮含量的预测模型最为理想。

关键词: 苹果, 光谱参数, 叶片全氮含量, 检测模型

中图分类号: 0433.1/TP79　　文献标识码: A

引用格式: 李丙智, 李敏夏, 周　璇, 张林森, 张海燕. 2010. 苹果树叶片全氮含量高光谱估算模型研究. 遥感学报, **14**(4): 761—773

Li B Z, Li M X, Zhou X, Zhang L S and Zhang H Y. 2010. Hyperspectral estimation models for nitrogen contents of apple leaves. *Journal of Remote Sensing*. **14**(4): 761—773

1　引　言

氮素是果树必需矿质元素中的核心元素, 作为养分与信号对果树的生长发育及产量品质的形成有重要影响, 在一定范围内其施用量与果树的产量、品质密切相关。为了追求高产、稳产, 生产中过量施肥, 甚至超量施肥现象较普遍, 但过量施氮不仅使硝酸盐在果品中积累增加, 产生食品安全问题, 而且造成硝态氮在土壤中积累, 污染生态环境。因此, 在保证果树优质丰产的前提下, 精准施氮技术就显得尤为重要。如何实时、快捷、准确地监测果树氮素营养, 及时指导果农科学施肥, 降低氮肥施用量, 提高氮肥利用率, 减少施氮环境污染, 已成为绿色果品生产需要解决的关键技术之一。

传统的叶片化学分析方法, 虽然对果树氮营养元素含量具有较高的检测精度, 但由于受高耗性、繁冗复杂性、时滞性等的制约, 不能大范围、快速地对果树营养进行诊断。随着高光谱遥感技术的快速发展与不断完善, 植被的遥感监测技术已涉及包括氮素在内的植株化学成分的估测, 并在理论和实践上为评价植物长势和生理参数特征提供了可靠的保证(Vane, 1993)。近年来, 随着高光谱遥感技术的快速发展与不断完善, 利用高光谱数据对各种植物的生化组分含量进行实时、快捷监测已成为可能。作物氮素的遥感监测一直是作物遥感监测研究的重点(Takebe, 1990)。Thomas 等(1972)进行了甜椒叶片的氮素与光谱反射率相关性测定, Yoder 等(1995)利用短波红外波段反射率进行对数变换以监测枫树叶片氮含量, Everitt 等(1987)提出波段反射率的比值可以监测杂草和花卉植物的氮素状况, Tarpley 等(2000)利用红边位置和短波近红外波段的比值预测棉花叶片氮浓度, Blackmer 等(1996)研究提出玉米氮素营养的敏感波段, Stone 等(1996)基于 671nm 和 780nm 两个波段反射率组合估算小麦植株全氮含量, 薛利

收稿日期: 2009-09-09; 修订日期: 2009-10-13

基金项目: 国家科技支撑计划(编号: 2007BAK31B01); 国家现代农业(苹果)产业技术体系; 农业部 948 项目(编号: 2006-G28)。

第一作者简介: 李丙智(1956—　), 男, 教授, 硕士, 1983 年毕业于西北农林科技大学园艺系, 目前主要从事果树生理与生态研究。已出版著作 23 部, 发表论文 28 篇。E-mail: bzhli530530@163.com。

红等(2004)利用660nm和460nm 两波段组合反映小麦叶片氮含量。可见，农作物氮素营养研究与遥感学科的交叉和融合已成为当前作物氮素营养研究领域一个重要研究方向，并且已成为该领域研究的热点。

前人利用高光谱数据对植物氮素含量进行定量化估测的研究较多(朱艳等, 2006; 王人潮等, 1993)。但对多年生果树氮素含量的定量化估测研究极少。如何在果树叶片这一小尺度上，利用光谱分析手段对其氮素含量予以精确的估测，对指导果树合理施肥具有重要意义。

本研究以不同年份、品种与施氮水平的田间试验为基础，对苹果鲜叶片的光谱反射率和全氮含量进行了测定。综合分析苹果叶片全氮含量与高光谱参数的关系，比较多种光谱参数估算叶片全氮含量的效果，以期确立叶片全氮含量的定量监测模型，为遥感技术在苹果氮素营养诊断中的实际应用提供理论依据和技术支持。

2　材料与方法

2.1　试验设计

为此，本研究进行了 3 个田间试验，涉及不同年份、品种类型及施氮水平。基本情况如下:

试验 **1**: 2007—2008 年在陕西省宝鸡市凤翔县苹果专家大院进行。供试土壤为沙壤土，有机质2.09%, 全氮 0.18%, 速效氮 120.20 $mg\cdot kg^{-1}$, 速效磷 110.03 $mg\cdot kg^{-1}$, 速效钾 83.5 $mg\cdot kg^{-1}$。试验因子分为品种和施氮量。供试品种为礼富一号和嘎拉; 施氮水平($kg\cdot hm^{-2}$), 分别为 0(N_1)、320(N_2)和 640(N_3)纯氮。试验共 6 个处理, 3 次重复，随机排列。氮肥的灌施分 3 次进行, 4 月份花期进行第 1 次灌施, 6 月份幼果生长期进行第 2 次灌施, 7 月份幼果膨大期进行第 3 次灌施。其他栽培管理措施同一般果园。分别在 5 月中旬、7 月中旬、9 月中旬和 10 月中旬进行苹果叶片光谱测定，并取对应叶片测定全氮含量。该试验资料用于监测模型的构建。

试验 2: 2007—2008 年在陕西省宝鸡市凤翔县范家寨乡范家寨村董贵转苹果园进行。供试土壤为砂壤土，有机质 1.43%, 全氮 0.11%, 速效氮 62.5 $mg\cdot kg^{-1}$, 速效磷 10.36 $mg\cdot kg^{-1}$, 速效钾 62.5 $mg\cdot kg^{-1}$。试验因子分为品种和施氮量。供试品种为红富士和秦冠; 施氮水平($kg\cdot hm^{-2}$), 分别为 0(N_1)、345(N_2)、690(N_3)纯氮。试验共 6 个处理, 3 次重复，随机排列。其他栽培管理措施同一般果园。田间光谱测试和采样日期与试验 1 相同。该试验资料用于监测模型的检测。

试验 3: 2007—2008 年在陕西省宝鸡市凤翔县范家寨乡张家沟村霍智文苹果园进行。供试土壤为沙壤土, 有机质 1.75 %，全氮 0.52 %, 速效氮 81.20 $mg\cdot kg^{-1}$, 速效磷 74.03 $mg\cdot kg^{-1}$, 速效钾 81.51 $mg\cdot kg^{-1}$。试验因子分为品种和施氮水平。供试品种为红富士和秦冠; 施氮水平($kg\cdot hm^{-2}$), 分别为 0(N_1)、345(N_2)、690(N_3)纯氮。试验共 6 个处理, 3 次重复，随机排列。其他栽培管理措施同一般果园。田间光谱测试和采样日期分别为: 5 月中下旬、7 月中旬、9 月中旬。该试验资料用于监测模型的检测。

2.2　光谱测定

采用美国 ASD(Analytical Spectral Device) 公司生产的 Field-Spec Pro 便携式光谱仪，波段范围为325—1075nm, 光谱采样间隔为 1.5nm, 光谱分辨率为 3.5nm。光谱的测定选择在天气晴朗、无云无风或风速很小时进行，测量时间为 10:00—14:00。选择树冠外围四周 50 个叶片进行测量，每个叶片测量 5 次。测量过程中，及时对观测前后的每组目标进行标准白板校正(标准白板的反射率为 1)，这样所测得的目标物光谱是无量纲的相对反射率。在具体测试过程中，对不同背景条件下(黑布、白纸、土壤)苹果叶片的光谱特性进行了测量和分析。苹果叶片的反射率在不同的背景条件下只是简单的平移，而这些通过光谱预处理技术便可消除(Min, 2008)。

2.3　叶片全氮的测定

采用 Tecator 凯氏定氮仪法测定叶片全氮浓度，将每个小区(7 株)试验树进行光谱测量后的叶片(350个叶片)，混合组成独立样品(每个测定时期 6 个处理，重复 3 次，共 18 个独立样品, 4 个采样时期共 72 个氮样品)，立即带回实验室，用蒸馏水将叶片洗净，在 105℃杀青 10—15min, 80℃下烘干。样品分别粉碎后，经过消煮、蒸馏后，进行滴定，通过下列公式计算氮含量。

$$含氮量=\frac{(V-V_0)\times C_H\times 0.014}{m}\times 100\%$$

式中，V 为滴定试液时所用酸标准溶液的体积(ml); V_0 为空白滴定时所用酸标准溶液的体积(ml); C_H 为酸标准溶液的浓度($mol\cdot L^{-1}$); m 为烘干叶片质量(g)。

2.4　数据分析

以试验 1 的数据为基础，对苹果叶片各项光谱

参数与叶片全氮含量进行相关分析，选择与叶片全氮含量显著相关的敏感波段及植被指数，并通过逐步回归分析确定监测苹果叶片全氮含量的最佳光谱指数，建立监测模型(浦瑞良&宫鹏，2000; Guyot & Baret, 1988; Richardson & Wiegand, 1977; Pearson & Miller, 1972)。

利用试验2和试验3的数据对以上监测模型进行测试与检验。模型的准确性和适用性采用通用的根均方误(RMSE)、相对误差(RE)和精度 (R^2) 3 个指标进行评定，并绘制预测值与观察值之间的 1∶1 关系图，以直观展示监测模型的拟合度和可靠性。

3 结果与分析

3.1 不同施氮水平对苹果叶片光谱的影响

以试验１礼富一号叶片７月中旬光谱反射率为例说明不同施氮水平下苹果叶片光谱反射率的响应模式(图 1(a))，并对礼富一号 N_2 处理生育期叶片光谱反射率作图，表达叶片光谱随生育时期的动态变化(图 1(b))。从图 1(a)看出，施氮水平的差异影响叶片光谱反射特征，在不同波段区域光谱响应不同。随施氮水平的增加，叶片光谱在可见光区 (400—710nm)的反射率均逐渐降低，而近红外波段(760—1000nm)的反射率均逐渐升高。其中叶片光谱反射率在可见光波段(510—620nm)形成一个明显的反射峰，在近红外波段(780—1000nm)有个明显的反射高台。同时，在这两个特征谱段，可以有效区分不同施氮水平。2 年试验的测定结果大体一致，不同品种之间的表现也基本相同。

对不同生育时期苹果叶片光谱的分析表明，生育期差异对光谱的影响与叶片全氮含量类似，具有明显规律性变化的波段区域主要在可见光波段 500—700nm 和近红外波段 750—1000nm 区域(图 1(b))。这是由于不同生育阶段叶片生物量和生化组分在变化，光谱也发生了相应的变化。因此，不同生育期的植株长势及生理变化对光谱产生重要影响，随着生长阶段的推进，叶片在可见光区的光谱反射率逐渐降低，在近红外区逐渐升高。

3.2 苹果叶片全氮含量与原始光谱反射率之间的关系

将试验 1 生育时期的叶片全氮含量与对应的光谱反射率及其一阶微分光谱数据 n=216 综合起来进行相关分析(图 2)。寻找苹果叶片敏感波段和建立普适性的叶片氮素监测模型。相关分析表明，叶片全

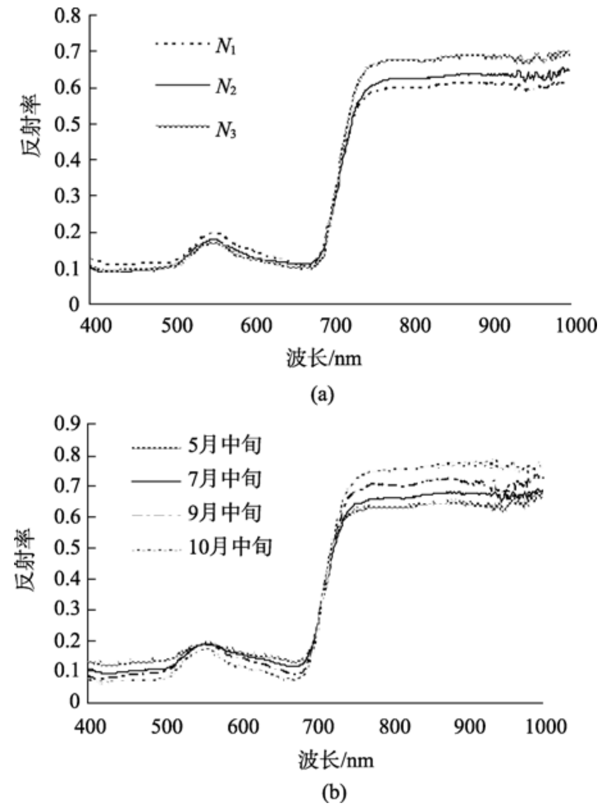

图 1 不同施氮水平的苹果叶片光谱(a)及生育期(b)的变化

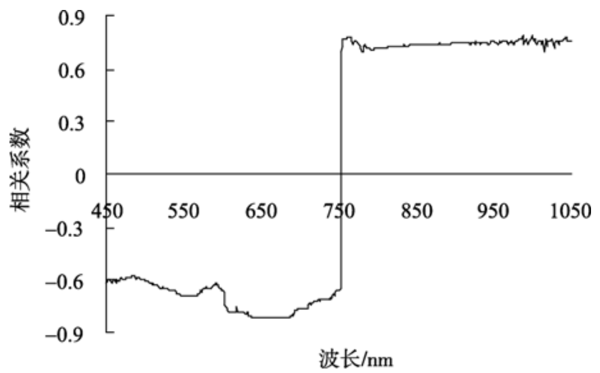

图 2 苹果叶片全氮含量与原始光谱的相关性

氮浓度与可见光波段(400—700nm)反射率呈极显著负相关，形成 650—700nm 的吸收峰，即红谷，是由于叶绿素 a/b 强烈吸收引起的，该波段对氮素比较敏感。在 760—1000nm 间相关系数形成一个较高的反射平台 r = 0.788，该区域光谱对叶面积和生物量反应敏感，由于叶片氮含量与叶面积和生物量等参数相关，这主要是不同施氮水平导致不同的生物量和叶面积指数。“红边”波段是可见光到近红外的过渡区域，已有研究发现，“红边”位置参数与植被叶绿素含量、叶面积指数、生物量等参数间存在显著的相关性。通过分析发现，两者之间在 715nm 处

具有最大相关系数($r = -0.817$)。

以全氮含量作为因变量，715nm 处的光谱反射率作为自变量，通过线性和非线性拟合分析建立全氮含量与这一波段处反射率的关系模型。从图 3 可见，对数模型与线性模型相比拟合效果相对较好，说明这一关系模型可对全氮含量进行较好的预测。

3.3　苹果叶片全氮含量与一阶微分光谱反射率之间的关系

叶片氮含量与一阶微分光谱之间相关分析(图 4)表明，在 550—600nm 为负相关且达较高水平，相关系数为 $r = -0.84$，此区域位于黄边范围。在 700—750nm 表现正相关，最大相关系数波长位于 723nm 附近，$r = 0.87$，达极显著水平，该处光谱急剧变化处于红边范围，与氮含量关系密切。红边区域蕴涵丰富的光谱信息，已报道许多光谱指数均与该区域有关，通过此区域光谱信息挖掘，对于估计与色素有关生化组分有意义。

以全氮含量为因变量，723nm 处反射率一阶微分为自变量，通过线性和非线性拟合分析建立两者之间关系模型。从图 5 可见，线性和非线性模型与全氮含量拟合效果接近。与原始光谱对全氮含量的

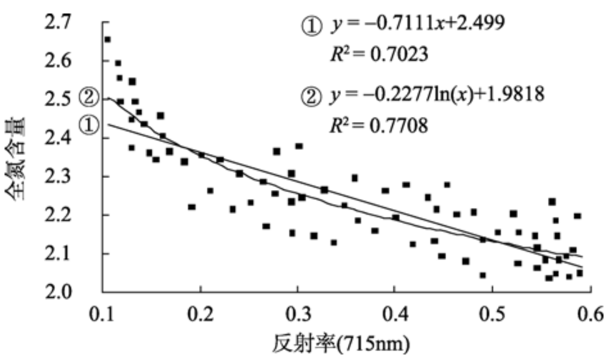

图 3　叶片全氮含量与特征叶片反射率(715nm)回归关系

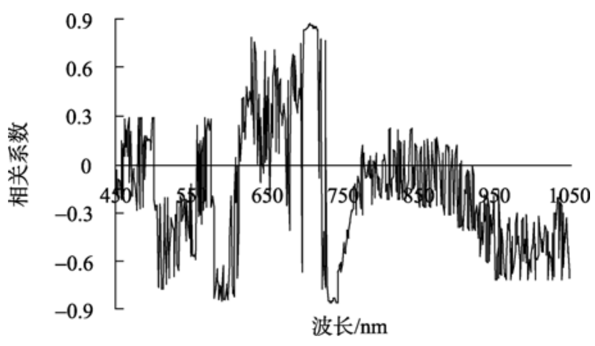

图 4　全氮与一阶微分光谱的相关性

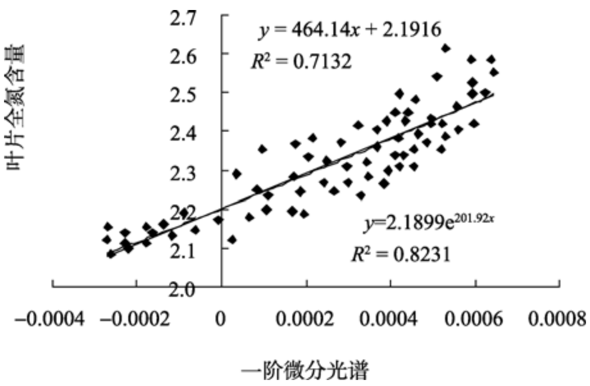

图 5　叶片全氮含量与特征叶片一阶微分光谱(723nm)的回归关系

线性和非线性拟合模型的判定系数相比，一阶微分与全氮含量的拟合程度不论是线性还是非线性的都相对较高，说明用反射率的一阶微分对全氮含量进行预测具有可行性。

3.4　苹果叶片全氮含量与高光谱参数的关系

表 1 为光谱参数的定义。

表 1　光谱参数的定义

类型	光谱参数	定义
基于光谱位置变量	Dr	红边内最大一阶微分值
	λr	Dr 对应波长
	Db	蓝边内最大一阶微分值
	λb	Db 对应波长
	Dy	黄边内最大一阶微分值
	λy	Dy 对应波长
	Rg	绿峰反射率
	λg	Rg 对应波长
	Ro	红谷反射率
基于光谱面积变量	SDr	红边内一阶微分总和
	SDb	蓝边内一阶微分总和
	SDy	黄边内一阶微分总和
基于植被指数变量	SDr/SDb SDr/Sdy Rg/Ro	比值植被指数
	(SDr−SDb)/(SDr+SDb) (SDr−SDy)/(SDr+SDy) (Rg−Ro)/(Rg+Ro)	归一化植被指数

从表 2 可见，“三边”光学参数中，除了黄边位置(λy) 与全氮含量没有达到极显著相关之外，其余三边位置变量与全氮呈极显著相关；绿色反射峰(Rg)，红光吸收谷(Ro) 以及 Rg 对应的波长(λg) 也与全氮含量达到极显著相关水平；“三边”面积变量也都与全氮含量具有较强的相关性，其中与蓝边面积变量相关性最强。基于植被指数的变量中，全

表 2 全氮含量与高光谱特征变量之间的相关系数

	光谱变量类型	相关系数(r)
基于光谱位置变量	Db	−0.855
	λb	0.752
	Dr	−0.818
	λr	0.876
	Dy	−0.830
	λy	0.147
	Rg	−0.808
	λg	0.721
	Ro	−0.741
基于植被指数变量	SDr/SDb	0.874
	SDr/SDy	−0.129
	Rg/Ro	−0.647
	(SDr−SDb)/(SDr+SD_b)	0.853
	(SDr−SDy/(SDr+SDy)	−0.256
	(Rg−Ro)/(Rg+Ro)	−0.641
基于光谱面积变量	SDr	−0.806
	SDb	−0.839
	SDy	0.725

氮含量除了与由红边面积和黄边面积所构建的比值植被指数和归一化植被指数的相关性较弱之外，与其他指数均呈极显著相关关系，说明采用这些变量对全氮含量进行估算具有可行性。全氮含量与高光谱特征变量之间具有很强的相关性，从这些变量中挑选出与全氮含量呈极显著相关的变量进行单变量线性和非线性拟合分析，建立方程，期望找出较适合于全氮含量估算的高光谱遥感模型。

从表 3 可见，基于三边幅值(Dr、Db 和 Dy) 所构建的线性和非线性的预测模型均是对数模型具有较大的判定系数，优于其他两类模型； 基于红边位置(λr) 所构建的各类模型与基于其他变量所构建的各类模型相比，具有最大的判断系数，与叶片全氮浓度的拟合结果最好。并且所构建的线性和非线性模型的拟合效果很接近。 但相比而言，线性模型具有较为简单的数学表达形式。因此，从这些变量中选取模型 y=43.391x−0.1467 对全氮含量进行预测，并对其预测精度进行检验。

3.5 叶片全氮含量估算模型的建立与检验

为了考察模型的可靠性和普适性，利用 2007—2008 年度独立数据 (试验 2 和试验 3) 对上述回归方程进行验证，采用通用的根均方误 (RMSE)、相对误差(RE)、精度 (R^2)、3 个指标检验模型的预测能力(表 4)，对检验结果较好的参数作 1∶1 关系图展示测试效果(图 6)。

表 3 苹果叶片全氮含量(**y**)与不同光谱参数(**x**)的定量关系(n=216)

光谱参数	模型	回归方程	R^2
Dr	线性	$y = -156.78x + 3.643$	0.649
	指数	$y = 4.854x^{-70.495}$	0.671
Db	线性	$y = 6.188x - 340.22$	0.720
	指数	$y = 4.357x^{-180.66}$	0.715
Dy	线性	$y = 3.022x - 2299.3$	0.737
	指数	$y = 3.195e^{-1256.3x}$	0.764
λr	线性	$y = 43.391x - 0.1467$	0.848
	指数	$y = 6.5e^{-0.027x}$	0.840
λb	线性	$y = -126.71x + 0.248$	0.523
	指数	$y = 6.8e^{-310.135x}$	0.534
Rg	线性	$y = 3.359x - 6761$	0.633
	指数	$y = 3.777e^{-361x}$	0.641
λg	线性	$y = 229.678x - 0.41$	0.472
	指数	$y = 1.4e^{-0.232x}$	0.542
Ro	线性	$y = 3.276x - 9648$	0.548
	指数	$y = 3.646e^{-5.218x}$	0.547
SDr	线性	$y = 3.802x - 4786$	0.672
	指数	$y = 4.781x^{-2.553}$	0.658
SDb	线性	$y = 3.088x - 11.021$	0.717
	指数	$y = 3.272x^{-5.892}$	0.705
SDr/SDb	线性	$y = 0.133x - 0.452$	0.765
	指数	$y = 0.590x^{0.2396}$	0.746
(SDr−SDb)/(SDr+SDb)	线性	$y = -2.113x - 6.614$	0.737
	指数	$y = 0.590x^{-0.2396}$	0.725

表 4 全氮含量高光谱估算模型的精度检验结果比较(n = 72)

自变量 x	模型表达式	R^2	RMSE	RE
ρ715	$y = -0.2277\ln(x)+1.9818$	0.771**	0.377	17.7
ρ723	$y = 2.1899e^{201.92x}$	0.879**	0.245	9.86
λr	$y = 43.391x - 0.14$	0.848**	0.302	12.46
SDr/SDb	$y = 0.133x - 0.452$	0.759**	0.370	16.78

注: *, **分别表示显著和极显著。

结果表明，这些变量均可对全氮变化进行较好的解释，但是考虑到一个变量可能对多个参数的变化响应，引起变量变化的参数不确定性，如红边波长 λr 和 SDr/SDb 也可对粗纤维和色素等的变化有响应，所以要求所选变量能对参数变化有较好的解释同时，还要求这一变量对参数变化解释的唯一性，基于以上原则再进行筛选，发现 715nm 处的原始光谱反射率和 723nm 处的一阶微分值符合要求，而采用 723nm 处的一阶微分值所构建的指数模型具有最大相关系数、最小 RMSE 和最小 RE，作为对全氮的预测模型最为理想。因此选取模型：y= $2.1899e^{201.92\rho723nm}$，作为全氮含量预测模型。

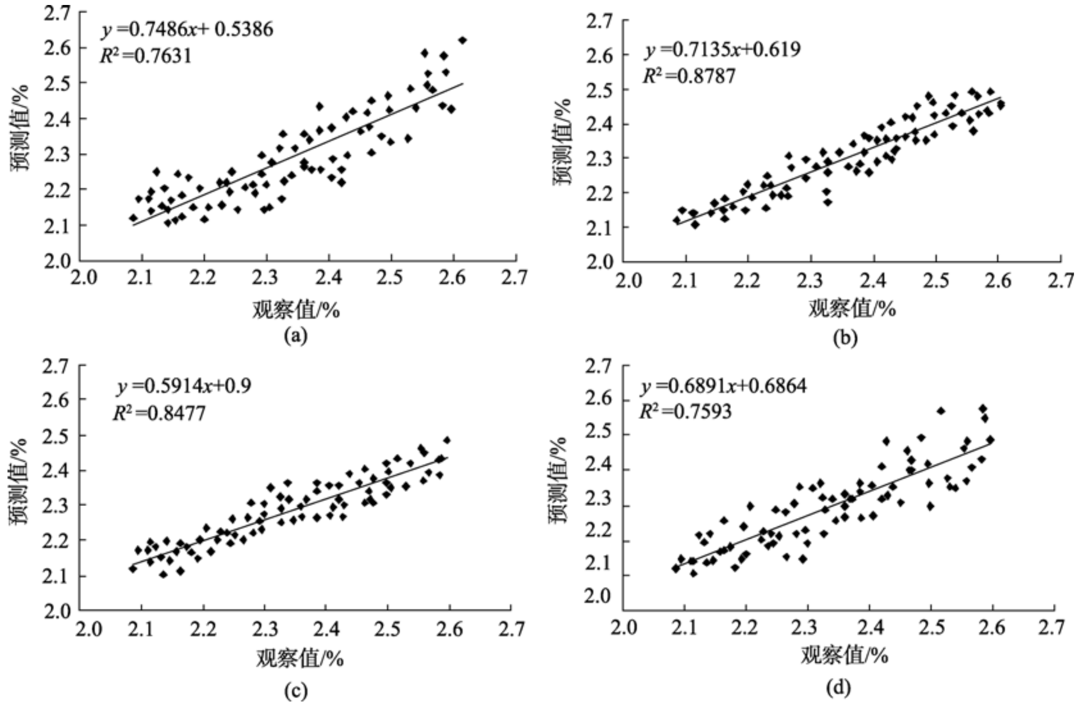

图 6 全氮含量预测值和实测值的比较

(a): 2007 年礼富一号; (b): 2007 年嘎拉; (c): 2008 年礼富一号; (d): 2008 年秦冠

4 讨 论

本研究采用苹果叶片全氮含量高光谱遥感分析估算，属于一种无损测试技术，即在不破坏植物叶片组织结构的前提下，利用光谱仪测得的叶片全氮光谱反射特征变化。与传统的室内生化分析方法相比，遥感方法不仅是活体观测，而且获得的是“面状”信息，使分析成本降低。本文综合分析了苹果叶片全氮含量与叶片光谱特征的定量关系，在研究氮素敏感波段的基础上，建立了基于红边位置(λr)的苹果叶片全氮含量监测模型。研究结果发现，两波段组合的光谱变量(尤其在对数处理后)与全氮拟和方程的拟合度比单一波段与之建立的方程的拟合度要大的多。说明多波段组合光谱变量更适合全氮含量的判别。这与 Daughtry 等(2000)研究的结果是一致的。原因可能是单一波段光谱反射率容易被背景反射或者叶面积指数的变异所混淆干扰。因此，应寻找对氮素敏感并且能使影响叶片或冠层反射的背景因素最小化的光谱指数来监测叶片氮素状况。为了准确地反应植株氮素营养状况，消除或减轻背景噪音的影响，人们不断提出和发展新的光谱指数。Rondeaux 等(1996)提出，OSAVI 可以降低土壤背景的干扰，从而反映作物的生长状况。“红边”位置波段(680—760nm)的光谱对叶面积和生物量反应敏感，由于植株氮含量驱动叶面积和生物量参数，因此该区域对氮含量也反应敏感。由于导数光谱在红边内存在，双峰红边内导数光谱的极大值所对应的波长位置(由定义求得)难免产生偏差且具有离散，Miller 等(1990)和 Cho 等(2006)分别利用倒高斯光学(IG)模型和线性外推法修正了红边位置。归一化处理可以消除观测背景的影响，突出“红边”位置包含的光谱信息。与已有的氮素敏感波段或植被指数相比，该指数综合了可见光波段的信息，容易获取，可为便携式氮素光谱监测仪的研制提供参考。

由于条件限制，本文所取光谱资料仅源于凤翔一个县，另外苹果产量与植株叶片叶绿素含量关系密切，今后应扩大取样地点，并设置不同产量和氮素水平，研究高光谱估计苹果产量的潜力，为高光谱技术在果园早日使用提供理论依据。

5 结 论

通过对全氮含量与高光谱反射率及其一阶微分以及高光谱特征变量和植被指数之间的关系分析可得出：施氮水平影响叶片光谱反射特征，不同波段区域光谱响应不同。随施氮水平的增加，叶片光谱在可见光区的反射率均逐渐降低，而近红外波段的反射率均逐渐升高。不同品种之间的表现基本相同。随着生长阶段的推进，苹果叶片在可见光区的光谱

反射率逐渐降低，在近红外区逐渐升高。苹果叶片全氮含量与原始光谱反射率之间在 715nm 处具有最大相关系数($r = -0.817$)。叶片全氮含量与一阶微分光谱之间的最大相关系数波长位于 723nm 附近，r=0.87，达极显著水平。所构建的非线性的对数关系模型对全氮含量的预测能力优于线性模型；对反射率的一阶微分，线性模型和非线性模型的预测能力接近，均可对全氮含量进行较好的预测。通过精度检验，综合分析采用723nm 处的一阶微分值所构建的指数模型作为对全氮的预测模型最为理想。

REFERENCES

Blackmer T M, Schepers J S and Varvel G E. 1996. Nitrogen deficiency detection using reflected short wave radiation from irrigated corn canopies. *Agronomy Journal*, **88**(1): 1—5

Cho M A and Skidmore A K. 2006. A new technique for extract in the rededge position from hyperspectral data: the linea extra polation method. *Remote Sensing of Environment*, **101**(2): 181—193

Daughtry C S T, Walthall C L and Kin M S. 2000. Estimatin corn leaf chlorophyll concentration from leaf and canop reflectance. *Remote Sensing of Environment*, **74**: 229—239

Everitt J H, Pettit R D and Alaniz M A. 1987. Remote sensing of broom snake weed (Gutierrezia sarothrae) and spinyaster (Astersposus).*Weed Science*, **35**(2): 295—302

Guyot G and Baret F. 1988. Utilisation dela haute resolutio spectrale poursuivrel'etatdes couverts vegetaux.Proceedings of the Fourth International Conference on Spectral Signatures of Objects in Remote Sensing, Assois(France): European Space Agency

Miller J R. 1990. Quantitative Characterization of the Vegetation Red Edge Reflectance.An Inverted Gauss Ian. Reflectance Model. *International Journal of Remote Sensing*, (11): 1775—1795

Min Min, Won Suk Lee, Thomas F Burks, Jonathan D Jordan, Arnold W Schumann, John K Schueller and Huikai Xie. 2008. Design of a hyperspectral nitrogen sensing system for orange leaves. *computers and electronics in agriculture*. **63**: 215—226

Pearson R L and Miller D L. 1972. Remote mapping of stand in crop biomass for estimation of the productivity of the shortgrass prairie. Proceedings of the Eighth Interntional Symposium on Remote Sensing of Environment. Michigan: Environmental Research Institute of Michigan

Pu R L and Gong P. 2000. Hyperspectral remote sensing and its application. Beijing: Higher Education Press

Richardson A J and Wiegand C L. 1977. Distinguishing vegetation from soil background information. *Photogramm Engineering and Remote Sensing*, **43**: 1541—1552

Rondeaux G, Steven M and Baret F. 1996. Optimization of soiladjusted vegetation indices. *Remote Sensing of Enviroment*, **55**: 95—107

Stone M L, Solie J B, Rrun W R, Whitneey W, Taylor S L and Ringer J D. 1996. Use of spectral radiance for correcting in-season fertilizer nitrogen deficiencies in winter wheat. *Transactions of ASAE*, **39**: 1623—1631

Takebe M, Yoneyama T, Inada K and Murakami T. 1990. Spectral reflectance ratio of rice canopy for estimating crop nitroge status. *Plant Soil*, **122**: 295—297

Tarpley L, Redd K R and Sassenrath Cole G F. 2000. Reflectance indices with precision. *Crop Science*, **40**: 114—119

Thomas J R and Oerther G F. 1972. Estimating nitrogen content of swepepper leaves by reflectance measurements. *Agronom Journal*, **64**: 11—13

Vane G. 1993. Terrestrial imaging spectro metry: Current status, future trends. *Remote Sensing of Environment*, **44**(2): 109—127

Wang R C, Chen M Z and Jiang H X. 1993. Study on the agricultural mechanism of yield estimation using remote sensing: Spectral characteristics of rice with different nitrogen level and selection of sensitive waveband. *Journal of Zhejiang Agricultural University*, **19**(Suppl): 7—14

Xue H L, Cao W X, Luo W H and Zhang X.2004.Correlation between leaf nitrogen status and canopy spectral characteristics in wheat. *Acta Phytoecologica Sinica*, **28**(2): 172—177

Yoder B J and Pettingew Crosby R E. 1995. Predicting nitrogen and chlorophyll concentrations from reflectance spectra (400—2500 nm) at leaf and canopy scales. *Remote Sensing of Environment*, **53**: 199—211

Zhu Y, Li Y X, Zhou D Q, Tian Y C, Yao X and Cao W X. 2006. Quantitative relationship between leaf nitrogen concentration and canopy reflectance spectra in rice and wheat. *Acta Ecologica Sinica*, **26**(10): 3463—3469

附中文参考文献

浦瑞良，宫鹏．2000．高光谱遥感及应用．北京：高等教育出版社

王人潮, 陈铭臻, 蒋亨显. 1993. 水稻遥感估产的农学机理研究——Ⅰ不同氮素水平的水稻光谱特征及其敏感波段的选择．浙江农业大学学报, **19**(增刊): 7—14

薛利红，曹卫星，罗卫红，张宪．2004．小麦叶片氮素状况与光谱特性的相关研究．植物生态学报, **28**(2): 172—177

朱艳，李映雪，周冬琴，田永超，姚霞，曹卫星．2006．水稻叶片氮含量与冠层反射光谱的定量关系．生态学报，**26**(10): 3463—3469